AD-A183 853 THEORETICAL ANALYSIS OF CHARGING DATA FROM ROCKET WITH CHARGED BEAM EMISSION(U) AIR FORCE GEOPHYSICS LAB HANSCOM AFB MA C W DUBS 02 OCT 86 AFGL-TR-86-0209 1/1

UNCLASSIFIED F/G 20/3 NL

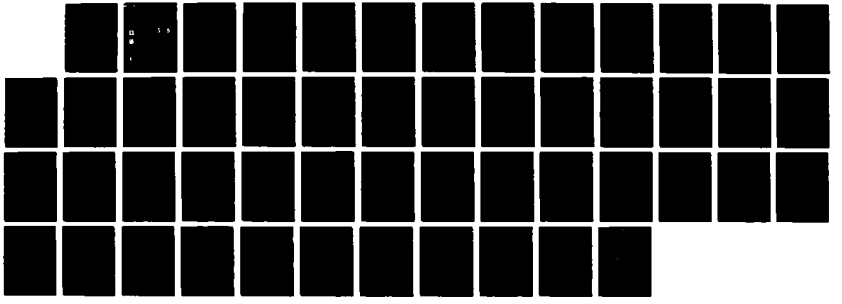

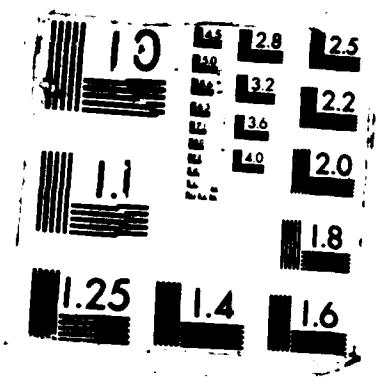
1.0
1.1
1.25
1.4
1.6
1.8
2.0
2.2
2.5
2.8
3.2
3.6
4.0

AFGL-TR-86-0209
ENVIRONMENTAL RESEARCH PAPERS, NO. 962

Theoretical Analysis of Charging Data From Rocket With Charged Beam Emission

CHARLES W. DUBS

2 October 1986

SPACE PHYSICS DIVISION PROJECT 7601
AIR FORCE GEOPHYSICS LABORATORY
HANSCOM AFB, MA 01731

Unclassified
SECURITY CLASSIFICATION OF THIS PAGE

AD-A183853

REPORT DOCUMENTATION PAGE

1a. REPORT SECURITY CLASSIFICATION Unclassified	1b RESTRICTIVE MARKINGS
2a. SECURITY CLASSIFICATION AUTHORITY	3 DISTRIBUTION / AVAILABILITY OF REPORT Approved for public release; distribution unlimited
2b. DECLASSIFICATION / DOWNGRADING SCHEDULE	
4. PERFORMING ORGANIZATION REPORT NUMBER(S) AFGL-TR-86-0209 ERP No. 962	5 MONITORING ORGANIZATION REPORT NUMBER(S)
6a NAME OF PERFORMING ORGANIZATION Air Force Geophysics Laboratory 6b OFFICE SYMBOL (If applicable)	7a NAME OF MONITORING ORGANIZATION
6c. ADDRESS (City, State, and ZIP Code) Hanscom AFB Massachusetts 01731	7b ADDRESS (City, State, and ZIP Code)
8a. NAME OF FUNDING / SPONSORING ORGANIZATION 8b OFFICE SYMBOL (If applicable)	9 PROCUREMENT INSTRUMENT IDENTIFICATION NUMBER
8c. ADDRESS (City, State, and ZIP Code)	10 SOURCE OF FUNDING NUMBERS PROGRAM ELEMENT NO: 62101F; PROJECT NO: 7601; TASK NO: 30; WORK UNIT ACCESSION NO: 01

11 TITLE (Include Security Classification)
Theoretical Analysis of Charging Data from Rocket with Charged Beam Emission

12 PERSONAL AUTHOR(S) Charles W. Dubs

13a TYPE OF REPORT	13b TIME COVERED	14 DATE OF REPORT (Year, Month, Day)	15 PAGE COUNT
Scientific, Interim	FROM _____ TO _____	1986 October	52

16 SUPPLEMENTARY NOTATION

17 COSATI CODES			18 SUBJECT TERMS (Continue on reverse if necessary and identify by block number)
FIELD	GROUP	SUB-GROUP	Potential coefficients, capacitance coefficients, potential, charges, rocket, beam current, return current, probe (continued on reverse)

19 ABSTRACT (Continue on reverse if necessary and identify by block number)

To gain physical understanding, an approximate analysis is made of charging data from the flight of a three-conductor rocket at night in the lower F-region of the ionosphere. Values of coefficients of potential, capacity, and induction are calculated, and a method of measuring them is given. Sheath radii are calculated. The extended probe is near the sheath's edge for 1 μA, and inside the sheath for all other (larger) beam currents. The potential of the rear section is calculated; it is near zero, and is negative. The other potentials follow from measurements of potential differences. Probe theory is used to calculate the plasma-return current to the forward section and is found to account for the high negative values of potential measured for unsaturated beam currents. The 374 μA and, especially, -10 mA beam-current cases are found to be highly saturated. Approximate formulae are developed to calculate the potential due to sheath charge. These, the coefficients, and the potentials give the conductor and sheath charges and the part of the conductor (continued on reverse)

20. DISTRIBUTION / AVAILABILITY OF ABSTRACT	21 ABSTRACT SECURITY CLASSIFICATION
☐ UNCLASSIFIED/UNLIMITED ☐ SAME AS RPT ☐ DTIC USERS	Unclassified
22a. NAME OF RESPONSIBLE INDIVIDUAL Charles W. Dubs	22b TELEPHONE (Include Area Code) 617-377-2931
	22c OFFICE SYMBOL PHK

DD FORM 1473, 84 MAR 83 APR edition may be used until exhausted
All other editions are obsolete

SECURITY CLASSIFICATION OF THIS PAGE
Unclassified

BLOCK 18 - SUBJECT TERMS (continued)

theory, sheath radii, charging time constant, conductors, probe position potential, theoretical analysis

BLOCK 19 - ABSTRACT (continued)

potentials due to the sheath. The charge on the forward section is nearly doubled due to the presence of the rear section. The potential at the position of the probe with the probe removed is calculated and found to differ greatly from the probe potential. The charging time constant due to rocket current and capacitances is an order of magnitude larger than the plasma period. The time to reach steady state is determined by the charging time constant due to capacitance for ion beam currents, and by the ion transit time for the electron beam current.

Contents

Illustrations

Tables

Acknowledgments

I thank our experimentalists for additional data, and my colleagues for helpful criticism. I am particularly grateful to Pradip Bakshi for reading several versions of manuscripts and for much helpful discussion.

NOMENCLATURE

Different meanings are separated by semicolons.

1	= conductor 1, forward section, also used as a subscript
2	= conductor 2, rear section, also used as a subscript
3	= conductor 3, extended probe, also used as a subscript
a	= radius of a sphere or a cylinder
A, A_n	= area, area of conductor n; Ampere
b	= half length of a cylinder
B	= half length of cylindrical sheath
c(a,b)	= capacitance of a conducting right circular cylinder a,b, Eq. (5)
c_{ij}	= coefficient of capacity or induction, element of matrix C, Section 3
C	= capacity; Coulomb
C	= 3 x 3 capacitance coefficient matrix, Section 3
C_f	= capacitance of the forward section by itself
C_f'	= capacitance of the forward section with the rear section attached, insulated, and uncharged
C_{fr}	= capacitance of the forward and rear sections attached and electrically connected

D = $p_{11}p_{22} - p_{12}^2$; determinant of P, Section 3

e = magnitude of electron charge; 2.718...; subscript refers to electrons

E = electric field

E_b = kinetic energy of beam particle

g = electrical conversion factor, $1/(4\pi\varepsilon_o)$ = 8.9876 m/nf

I_b = beam current leaving forward section

I = net (ion and electron) current from plasma to conductor

I_n = current from plasma (excluding beam particles) returning to conductor n

I_{nvm} = conventional voltmeter current from conductor n to 1, Section 4

k = Boltzmann constant when multiplied by T; otherwise 1.777

m = mass

m_e = mass of an electron

m_i = mass of an ion

n_o = ambient electron or ion number density

p_{ij} = coefficient of potential, element of matrix P, Section 3

p_{103} = value p_{13} would have if conductor 2 were missing

p_{123} = value p_{13} would have if conductor 1 and 2 were connected

P = 3 x 3 potential coefficient matrix, Section 3

q = electric charge

q_i = charge on conductor i, element of Q; instantaneous charge on i, Section 4.10

q_s = charge in the sheath

Q = 3 x 1 column charge matrix

r = spherical radial coordinate

r_c = ratio of charge on conductor 1 to that on 2 when both are at the same potential

R = (usually cylindrical) radial coordinate

R_s = sheath radius

t = time

t_t = initial ion traverse time through the sheath, Section 4.11

V = potential; Volt

$\mathbf{V}$ = 3 x 1 column potential matrix, Section 3

V_i = potential of conductor i, element of matrix V

$\mathbf{V}_s$ = 3 x 1 column matrix of conductor potentials due to sheath, Section 3

V_{is} = part of V_i that is due to the sheath charge, element of $\mathbf{V}_s$

z = cylindrical axial coordinate

Z_{i1} = resistance of voltmeter between conductors i and 1

δ = mean number of secondary electrons per primary incident particle, Section 4

ξ = ratio of conductor radius to Debye length

ρ = net electrical charge density

τ = charging time constant of conductor 1 due to currents and capacitance, Section 4.8

ϕ_{i1} = $V_i - V_1$

χ = eV/kT

Theoretical Analysis of Charging Data From Rocket With Charged Beam Emission

1. INTRODUCTION

The emission of an ion or electron beam from a spacecraft into the ambient plasma changes the potential on the beam-emitting section and, by induction, on other parts of the spacecraft relative to that of the ambient plasma. The values of the resulting potentials depend on the parameters of the beam, rocket, and plasma. Since this dependence was not well-known, Cohen et al.[1] carried out an experiment with a rocket in the lower F-region of the ionosphere at night. Potential differences between pairs of three isolated conductors were measured when a positive ion or electron beam was emitted from one of them. These voltages seemed remarkably high, even for relatively low positive beam currents. Questions arose as to why some of the measured values resulted. This report analyzes some of the data to try to answer the questions, and to gain further understanding of the results. After the original analysis,[2] Katz and Mandell[3]

(Received for publication, October 1986)

1. Cohen, H. A., Sherman, C., and Mullen, E. G. (1979) Spacecraft charging due to positive ion emission: an experimental study, G.R.L. 6:5-15.

2. Dubs, C. (12 Nov. 1982) Potentials and Charges on Conducting Rocket Sections, AFGL-TR-82-0349, ADA130143.

3. Katz, I., and Mandell, M. J. (1982) Differential charging of high-voltage spacecraft: the equilibrium potential of insulated surfaces, J.G.R., 87:4533-4541.

issued a paper that contains some analysis of this experiment. These analyses are compared. This report is a revision and an extension of the original analysis.

In this report, "ion" means "positive ion." Section 2 outlines the experiment and lists the data analyzed here. Values of coefficients of potential, capacity, and induction are determined in Section 3. They contribute physical insight, including the charge on each conductor and in the sheath, the potential of the position of the probe if the probe was removed, and the charging time constant due to capacitance and currents. For any configuration, these coefficients depend only on the geometry. For sufficiently simple geometry, they can be calculated, as is done in this case, without direct use of potential theory. How they can be measured before or after flight for verification, or in lieu of calculation for any geometry and number of conductors, is outlined. In Section 4, the absolute potentials of the rocket conductors, charges on them, sheath parameters, probe position potential, time constants for steady state, etc., are determined from the given parameters. Useful empirical formulae are also given for the theories of Laframboise, Langmuir-Blodgett, and Lam. Discussion includes the charge and potential behavior after the beam is turned on, comparison of measured currents with those calculated from probe theory, secondary electrons, sense of surface charge densities, saturation phenomena, and the effect of voltmeter resistance. The conclusions are summarized in Section 5.

2. EXPERIMENT

Cohen et al.[1] flew a rocket with three conductors insulated from each other: forward section, 1, rear section, 2, and extended thermal emissive probe, 3 (see Figure 1 and Table 1) to 258 km altitude at night. Conductors 1 and 2 were coaxial cylinders separated by an insulating ring. Conductor 3 was a sphere and a short, thin, hot wire filament (not shown). At certain times, an ion or electron beam of known current, I_b, and particle energy, E_b, was emitted from the front of the forward section, causing certain steady-state potentials and charges to develop on the three conductors. Voltmeters measured $\phi_{21} = V_2 - V_1$ and $\phi_{31} = V_3 - V_1$. The numbers in Table 2 are the part of the results, nine cases, that are analyzed here. The value of I_b designates the case. The plasma density was near 10^9 m^{-3} and the temperature, T, of both ions and electrons was near 550°K, so these values are assumed here. The potentials were measured after steady state was reached, so the return current from the plasma, minus secondary electron current, plus returning beam current if above saturation

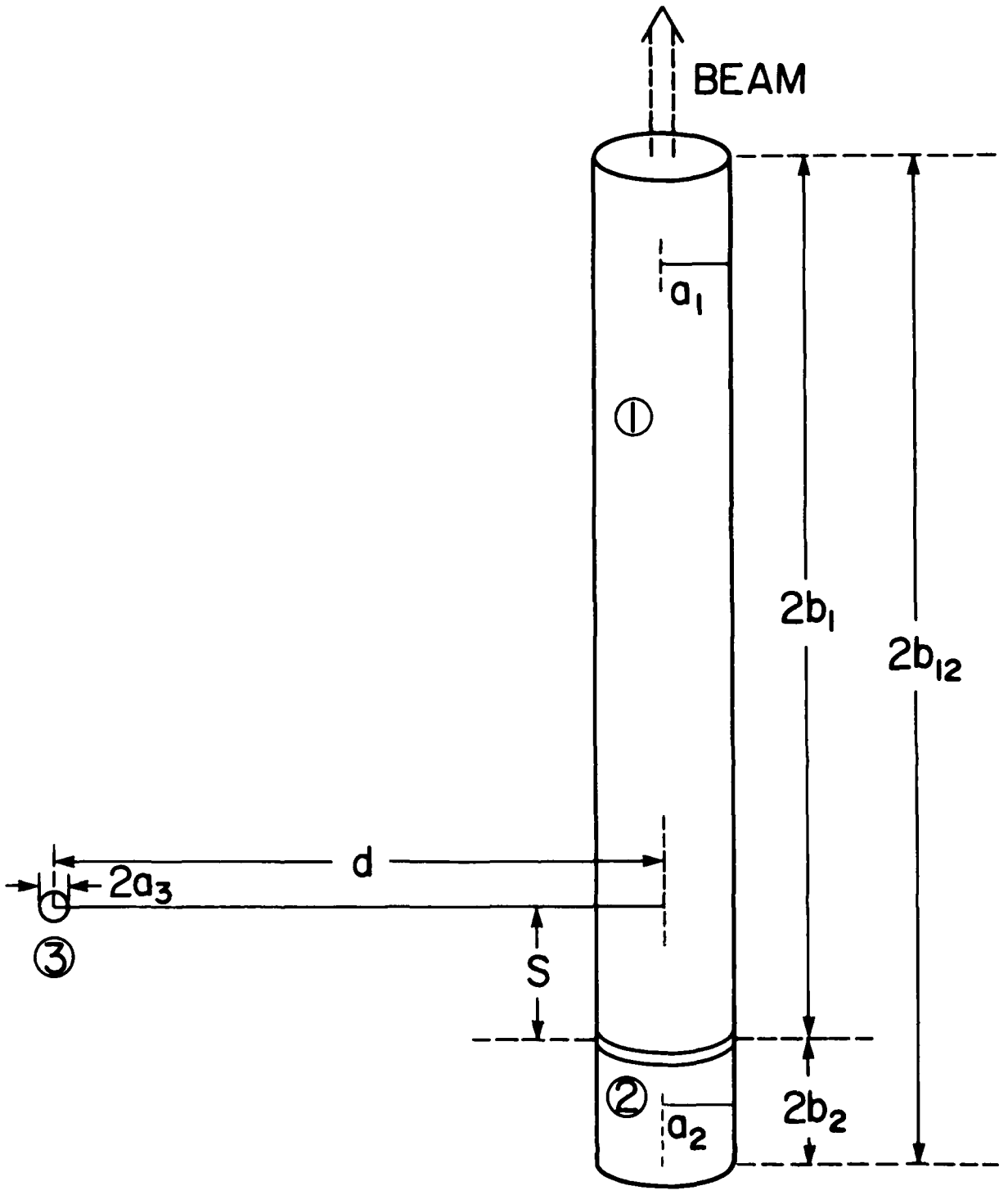

Figure 1. Rocket Configuration

Table 1. Rocket Dimensions in Meter

a_1	a_2	a_3	b_1	b_2	b_{12}	s	d
.19	.19	.019	1.27	.205	1.475	.26	1.71

Table 2. Measured Beam Current and Energy, Rocket Altitude, and Conductor Potential Differences

Beam	Ion	Ion	Ion	Ion	Ion	Ion	Ion	Ion	Electron	
I_b	1	8_a	8_b	8_c	9	10.9	12	374	-10^4	μA
E_b	.2	1	1	1	1	2	2	2	.09	keV
Cohen et al.	Table 1	Fig. 4	Fig. 3	Fig. 3	Table 1	Fig. 5	Table 1	Fig. 5	Table 1	
Altitude	158		153	138	163		161		160	km
ϕ_{21}	50	580	423	506	420		550		-90	V
ϕ_{31}	20	339	291	370	250	470	340	1,040	-90	V

(Section 4), equals I_b, and electrostatic theory is used, except for charging and ion transit times. An ion beam was emitted with the electron beam, but its current was negligibly small; thus, it is ignored in the "electron" column of Table 2. At least for ion-beam emission, the data were found to be independent of pitch angle and neutral number density. For this reason, as well as for simplicity, the magnetic field and neutral density are ignored in the analysis. The effect of ram

is neglected since the rocket orientation is unknown, but it should be important for ion current. Questions arose: What were the absolute values of the potentials? Why was $\phi_{31} \leq \phi_{21}$? The purpose of this report is to make an approximate analysis of the measurements in Table 2, and to gain an understanding of some of the basic electrical phenomena, as well as to try to answer these questions.

3. COEFFICIENTS OF POTENTIAL, CAPACITY, AND INDUCTION

The purpose of this section is to determine values of the coefficients of potential, capacity, and induction for the three conductors of the rocket system. These coefficients relate the charges to the potentials on these conductors. Since they were not measured, they are calculated. Fortunately, the geometry is simple enough so that it is not necessary to start from potential theory. The coefficients are obtained by using Smythe's formula[4] for the capacitance of a conducting right circular cylinder, an empirical formula found for the potential at a point near such a charged cylinder, carrying out three gedanken experiments, and interpolating.

Let p_{ij}, c_{ii}, and c_{ij} for $i \neq j$ be the coefficients of potential, capacity, and induction, respectively, the elements of matrices P and C. From electrostatics, e.g., a slight generalization of Page,[5]

$$V = PQ + V_s, \tag{1}$$

$$Q = C(V-V_s), \tag{2}$$

$$C = P^{-1}, \tag{3}$$

P and C are symmetric, the p_{ij} and c_{ii}'s are positive, and the c_{ij}'s for $i \neq j$ are negative. V_s accounts for the effect of the plasma.

Physical reason leads to the inequality of rocket capacitances

$$C_f < C_f' < C_{fr}. \tag{4}$$

Smythe[4] gave the following empirical formula (here slightly modified to make it correct within .30% instead of .41%) for the capacitance of a conducting right circular cylindrical conductor of radius a and half-length b for $a/8 \leq b \leq 8a$:

---

4. Smythe, W. R. (1962) Charged right circular cylinder, J. Appl. Phys. 33:2966-2967.

5. Page, L. (1935) Introduction to Theoretical Physics, Second Edition, § 120.

$$c(a,b) = [.0707 + .0615(b/a)^{.76}]a \text{ nf}, \tag{5}$$

a and b in meter. In particular, from this and Table 1,

$$C_f = .0629 \text{ nf} \tag{6}$$
$$C_{fr} = .0689 \text{ nf}. \tag{7}$$

Three gedanken experiments, designated with the subscripts a, b, and c, are now carried out in a vacuum. Eq. (1) with $V_s = 0$ is used for each. In the first experiment, charge q_{1a} is put on 1 while 2 and 3 are left uncharged. Then

$$V_{1a} = p_{11}q_{1a} \tag{8}$$
$$V_{2a} = p_{12}q_{1a} \tag{9}$$
$$V_{3a} = p_{13}q_{1a}. \tag{10}$$

When uncharged, 3 is small and far away enough from 1 and 2 to affect their potentials negligibly, so

$$q_{1a} = C_f'V_{1a}' \tag{11}$$

and

$$p_{11} = 1/C_f'. \tag{12}$$

Physical consideration shows that $|V_{2a}| < |V_{1a}|$, so Eqs. (8) and (9) show that

$$p_{12} < p_{11}. \tag{13}$$

In the second experiment, charge q_{1b} is put on 1 and q_{2b} on 2 such that $V_{1b} = V_{2b}$ with no charge on 3. Then

$$V_{1b} = p_{11}q_{1b} + p_{12}q_{2b} \tag{14}$$
$$V_{1b} = p_{12}q_{1b} + p_{22}q_{2b} \tag{15}$$
$$V_{3b} = p_{13}q_{1b} + p_{23}q_{2b}. \tag{16}$$

Again, 3 is small and far away enough so that

$$V_{1b} = (q_{1b} + q_{2b})C_{fr}^{-1} \tag{17}$$

accurately. This and $q_{1b} = r_c q_{2b}$ are substituted into Eqs. (14) and (15). The former may then be written

$$p_{12} = (r_c + 1)C_{fr}^{-1} - r_c p_{11}. \tag{18}$$

Substituting this into the latter leads to

$$p_{22} = r_c^2 p_{11} - (r_c^2 - 1)C_{fr}^{-1}. \tag{19}$$

How is r_c obtained? Smythe[4] expressed the surface-charge density of a charged conducting right circular cylinder as fractional power series, in z for the side, and in R for the ends (inner cylinder, Figure 2). He obtained the coefficients for several values of b/a. The coefficients for this ratio equals 8 are used since $b_{12}/a_1 = 7.76$. q_1 and q_2 are obtained by integrating these surface densities over 1 and 2 separately. The ratio gives

$$r_c = 3.770 \tag{20}$$

Details of this calculation are in Reference 2, Section A1. Thus, p_{11}, p_{12}, and p_{22} may be obtained given C_f'.

From Eq. (10),

$$p_{13}^{-1} = q_{1a}/V_{3a}. \tag{21}$$

The value p_{13}^{-1} would have if 2 were missing is shown in Appendix A and is given by Eq. (A5),

$$p_{103}^{-1} = .260_5 \text{ nf}. \tag{22}$$

Since 3 is small and far enough away, if 1 and 2 were electrically connected, p_{13}^{-1} would be

$$p_{123}^{-1} = \frac{q_{1b} + q_{2b}}{V_{3b}}, \tag{23}$$

Eq. (A6), Appendix A. Physical reason shows that

$$p_{103}^{-1} < p_{13}^{-1} < p_{123}^{-1}, \tag{24}$$

similar to Eq. (4). V_{3b} from Eq. (23) and $q_{1b} = r_c q_{2b}$ are substituted into Eq. (16), yielding

$$p_{23} = (r_c + 1)p_{123} - r_c p_{13}. \tag{25}$$

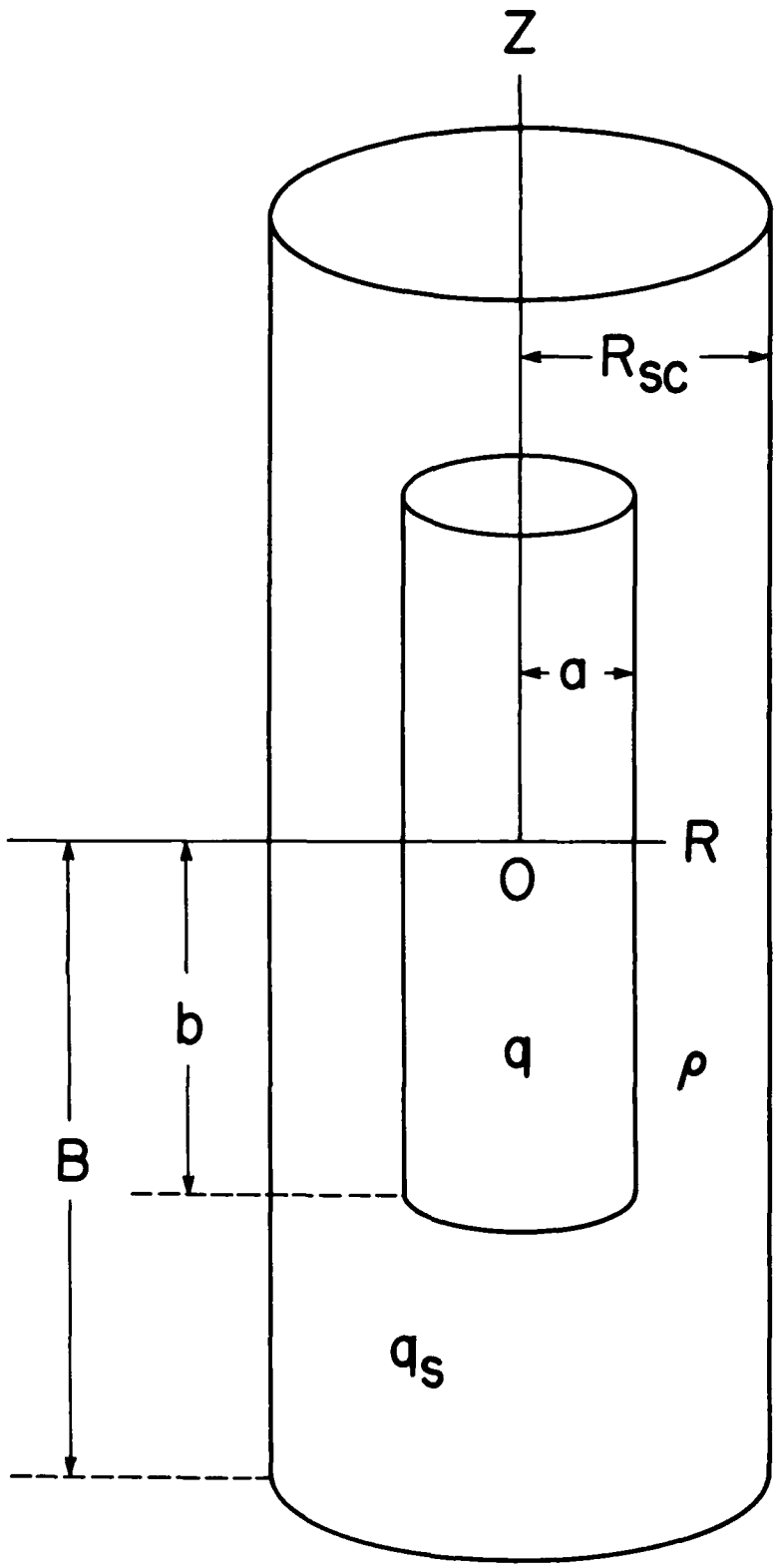

Figure 2. Cylinder With Cylindrical Sheath

In the third experiment, charge q_{3c} is put on 3 with no charge on 1 or 2. Then

$$V_{3c} = p_{33}q_{3c}. \tag{26}$$

A maximum effect calculation shows that the presence of 1 and 2 changes V_{3c} by less than .1%, so this effect is neglected. Therefore, $q_{3c} = C_3V_{3c}$, where the capacitance of 3 is $C_3 = a_3/g + C_w$, where C_w is the capacitance of the hot wire. For the wire, 2a = .00381 cm, 2b = 3.175 cm, so C_w = .0002620 nf, obtained for q/V from Eq. (A1) with R = a and z = 0, Appendix A. (It could also be obtained from the formula for the capacitance of a wire, the diameter of which, 2a, is small compared to its length, $b/[g\ \ln(b/a)]$ = .0002625 nf. Smythe's formula, Eq. (5), cannot be used since it does not reduce to the latter for b >> a). This is 11% of C_3. So, from the value of a_3 in Table 1,

$$p_{33} = 420\ (\text{nf})^{-1}. \tag{27}$$

Thus, all p_{ij}'s may be obtained given C_f' and p_{13}^{-1}.

With Eqs. (4) and (24) in mind, the value $b_1 + b_2/2$ of effective half-length of conductor 1 due to 2 being present, and the average of p_{103}^{-1} and p_{123}^{-1} for p_{13}^{-1} are chosen. Then

$$C_f' = c(a_1,\ b_1 + b_2/2) = .0659_5\ \text{nf}, \tag{28}$$

and

$$p_{13}^{-1} = .261\ \text{nf}. \tag{29}$$

These result from using the values in Table 1, Eqs. (5), (22), and (23). The value in Eq. (28) accurately equals the average of the values in Eqs. (6) and (7). From the above,

$$P = \begin{bmatrix} 15.2 & 12.1 & 3.83 \\ 12.1 & 23.7 & 3.79 \\ 3.83 & 3.79 & 420 \end{bmatrix} (\text{nf})^{-1} \tag{30}$$

These values should be correct within 5%, assuming negligible errors in the numbers in Table 1. From Eqs. (3) and (30),

$$C = \begin{bmatrix} 111. & -56.2 & -.503 \\ -56.2 & 70.7 & -.126 \\ -.503 & -.126 & 2.39 \end{bmatrix} \text{ pf.} \tag{31}$$

Ignoring 3, a good approximation,

$$c_{11} = p_{22}/D, \tag{32}$$

$$c_{12} = c_{21} = -p_{12}/D, \tag{33}$$

$$c_{22} = p_{11}/D, \tag{34}$$

$$D = p_{11}p_{22} - p_{12}^2 = (r_c + 1)^2 C_{fr}^{-1} \left[C_f'^{-1} - C_{fr}^{-1}\right]. \tag{35}$$

Choosing $q_2 = -q_1$, the capacity between 1 and 2 is

$$q_1/(V_1 - V_2) = 1/(p_{11} - 2p_{12} + p_{22})$$

$$= (c_{11}c_{22} - c_{12}^2)/(c_{11} + 2c_{12} + c_{22}) = 1/(C_{fr}D). \tag{36}$$

So, as the gap between 1 and 2 approaches 0, this capacity and $|c_{ij}|$ become very large since C_f' approaches C_{fr}. Including 3, as C_f' approaches C_{fr}, D approaches 0 and p_{13} approaches p_{123}.

Since the value of C_f' can be critical, the question naturally arises, "How reasonable is Eq. (28)?" Rocket sections 1 and 2 were separated by a 2-inch thick cylinder of fiberglass that was essentially hollow except for a one-half-inch thick fiberglass disc. To check, the capacitance between the two ends of an 18.7 cm length of the rocket that included the gap was measured and found to be 44.7 pf. A correction due to the missing lengths of 1 and 2 is calculated to be 10.2 pf. Adding this and equating to Eq. (36), D is obtained, which from Eq. (35) leads to C_f' = .0653 nf, insensitive to the value of capacity between 1 and 2, close to the value in Eq. (28).

These calculations of P can be checked or replaced by six measurements of capacity by hanging the rocket over 10 times its largest dimension (for < 5% error) from comparable and larger size conductors and ground, and running a small ground wire, 0, to the vicinity of the rocket. Measurement of the capacities between 1 and 0, 2 and 0, and 3 and 0 give the p_{ii}'s. Measurement of the capacities between 1 and 2, 2 and 3, and 3 and 1 give the p_{ij}'s for $i \neq j$. How this may be generalized to any number of conductors is evident.

4. NUMERICAL RESULTS

This section contains calculations of numerical values of at least ten types of physical quantities and a discussion of them. Unlike Reference 2, probe theory is used. Where applicable, calculated results are compared with experiments, and deductions are compared to those of Katz and Mandell.[3]

4.1 Absolute Potentials

First, the potentials, V_i, of the three conductors relative to that of the ambient plasma are calculated. This is done by determining the values of V_2, then using the measured values of ϕ_{i1} from Table 2. In Reference 2, it was assumed that $V_2 = 0$. V_2 must be sufficiently negative to attract a return current equal to the voltmeter current, $I_2 = \phi_{21}/Z_{12}$, plus net current due to secondary electrons. The latter current is neglected, but it could be important. $Z_{12} = 10^9\ \Omega$.

The formulas used here that relate the return current, I, due to ions, I_i, and to electrons, I_e, from the surrounding plasma to a conductor at a negative potential V, are the following:

$$\chi = \chi(i_i) \tag{37}$$

$$i_e = e^{\chi} \tag{38}$$

$$i_i = \frac{I}{I_{io}} + \sqrt{\frac{m_i}{m_e}}\, i_e \tag{39}$$

$$I = I_i + I_e \tag{40}$$

$$I_i = I_{io} i_i \tag{41}$$

$$I_e = I_{eo} i_e \tag{42}$$

$$I_{io} = n_o e v_{ti} A \tag{43}$$

$$I_{eo} = -\sqrt{\frac{m_i}{m_e}}\, I_{io} \tag{44}$$

$$V = \frac{kT}{e}\,\chi. \tag{45}$$

$$v_{ti} \equiv \sqrt{\frac{kT}{2\pi m_i}} \tag{46}$$

Eq. (39), (40), (41), (42), or (44) is redundant. $T_e = T_i = T$ is assumed since ion and electron temperatures are nearly the same in this experiment.

Since Table 1 shows a_2 and b_2 to be nearly equal, spherical probe theory is used for Eq. (37) to determine V_2. The effect of V_1 on I_2, the current to 2, is neglected. Probably V_1 being negative only cuts down the electron collecting area, affecting only the 1 μA case. For I_b = 1 μA or -10 mA, $|V_2|$ is small enough for the results of Laframboise[6] to apply. For $\xi < 5$, the following fit to Table 5c of Laframboise[6] is used:

$$-\chi = k_1(i_i - 1) + \frac{1 - k_1}{k_2} \ln[1 + k_2(i_i - 1)] \tag{47}$$

$$k_1 = 1 + \frac{6.83\xi - .685\xi^2}{(5 - \xi)^{1.7}} \tag{48}$$

$$k_2 = .0051\xi(5 - \xi)^{1.7} \quad . \tag{49}$$

These have an error of less than 1% for $\xi < 1$, 2% for $\xi < 3$, and 4% for $\xi < 5$. Interpolated correction factors are used so that the error is cut to ~ .2%. A more accurate interpolation and extrapolation for $\xi \lesssim .5$ is given in Section 4.9. $I = I_2$, and the conductor area, A, and radius, r_2, are chosen to satisfy $A = 4\pi r_2^2 = 4\pi a_2 b_2 + \pi a_2^2$. $\xi = 4.28$. The results are $|V_2|$ in the I_b = 1 and -10^4 μA columns of Table 3. For each of the other values of beam current, $|V_2|$ is so large that i_e is negligible, so is set equal to zero in Eqs. (38) to (42), and χ is out of the range of Laframboise's results. For them, Lam's[7] "highly negative" spherical probe potential theory is used for Eq. (37). (The Langmuir-Blodgett[8] formula for V is $(4/\pi)^{1/3}$ times the Lam formula with the argument of F multiplied by 1.26 (larger unless $\xi^2 j \gg 16$), so it gives larger values for $|V_2|$. It is not used since it disagrees much more with values extrapolated from Laframboise's results, and since it leads to currents further from experimental values.)

---

6. Laframboise, J. G. (1966) Theory of spherical and cylindrical Langmuir probes in a collisionless, Maxwellian plasma at rest, UTIAS Report No. 100.

7. Lam, S. H. (1965) Unified theory for the Langmuir probe in a collisionless plasma, Phys. Fluids 8:73-87.

8. Langmuir, I. and Blodgett, K. B. (1924) Currents limited by space charge between concentric spheres, Phys. Rev. 24:49-59.

Table 3. Forward and Rear Section Currents and Potentials

I_b	1	8_a	8_b	8_c	9	10.9	12	374	-10^4	μA
E_b	200	1,000	1,000	1,000	1,000	2,000	2,000	2,000	90	eV
I_2	.05	.58	.423	.506	.42	.483	.55	1.96	-.09	μA
I_b-I_2	.95	7.42	7.58	7.49	8.58		11.45	372	-10^4	μA
I_{1Lam}	2.58	11.7	9.57	10.7	9.53	10.4	11.3	25.8	-853	μA
V_1	-50	-588	-428	-512	-425	-489	-557	-2,000	90	V
V_2	-.26	-7.7	-4.7	-6.3	-4.7	-5.8	-7.1	-43	-.15	V
V_3	-30	-249	-137	-142	-175	-19	-217	-960	-.15	V

$$\chi = -\left[\frac{\xi^2 I_i}{4 I_{io}}\right]^{2/3} F\left(\sqrt{\frac{j}{j_m}}\right) \tag{50}$$

$$j = \frac{I_i}{\sqrt{1 + \frac{4}{\pi} I_{io}}} \tag{51}$$

$$j_m = 1.056 + 3.19(\xi^2 j)^{-2/5}. \tag{52}$$

These are valid for $\xi >> 1$, and for the argument of F large compared to $1 + \xi^{-1}$.

$$F(x) = \left[\frac{9}{4}(-\alpha)^2\right]^{2/3} \tag{53}$$

where $(-\alpha)^2$ as a function of $x = r_o/r$ is given by Langmuir and Blodgett.[8] The following empirical formula found for F is correct within 1%:

$$F(x) = \frac{(1.5\epsilon)^{4/3} + 1.28\epsilon^3}{1 + .44\epsilon + .67\epsilon^2} \tag{54}$$

$$\epsilon = x - 1. \tag{55}$$

Given F, ϵ from Eq. (54) is correct within 2/3% for $0 < \epsilon < 1$. The resulting values of V_2 for I_b = 8, 9, and 12 μA are in Table 3. How the values are obtained for I_b = 10.9 and 374 μA is explained later. The values of V_1 and V_3 in Table 3 follow from Table 2.

The values of V_2 are seen to be relatively close to zero. This is to be expected since Z_{21} is large. After an ion (electron) beam is turned on, the positive (negative) charge removal causes an increasing negative (positive) charge on 1 that induces a negative (positive) potential on 2. Thus, both sections attract return ions (electrons) from the plasma. In steady state, 1 must be sufficiently negative (positive) to attract a return current equal to the beam current minus the secondary electron current, here neglected, minus I_2. Conductor 2, however, must be only negative enough to attract a return current to cancel voltmeter and secondary electron current from 1 to 2. The secondary electron current, here neglected, effectively decreases Z_{21} making V_2 more negative. So, q_1 and q_2 must induce nearly equal but opposite potentials on 2. The sign of q_2 is the same as that of the beam particles, opposite to that of q_1, and $|q_2| < |q_1|$.

4.2 Return Current to Forward Section

Lam's[7] "highly negative" cylindrical probe potential theory is used to calculate the return current from the plasma to 1, $I_1 = I_{1Lam}$, from each value of V_1 in Table 3.

$$\chi_1 = -\left[\frac{\zeta^2}{2\sqrt{\pi}} \frac{I_j}{I_{10}} \frac{j}{j_m}\right]^{2/3} G\left(\frac{j}{j_m}\right) \tag{56}$$

$$\frac{j}{j_m} = \frac{\pi}{2\sqrt{4 + \pi .943}} \frac{I_1}{I_{10}} = \frac{1}{1.60} \frac{I_1}{I_{10}} . \tag{57}$$

$$G(x) = \left[\frac{9}{4} \frac{(-\beta)^2}{x}\right]^{2/3} \tag{58}$$

where $(-\beta)^2$ as a function of $x = r_o/r$ is given by Langmuir and Blodgett.[9] An empirical formula found for G correct to 1% is

$$G(x) = \frac{(1.5\gamma)^{4/3} + .869\gamma^3}{1 + .271\gamma + .417\gamma^2} \tag{59}$$

$$\gamma = \ln x. \tag{60}$$

(This γ is the negative of Langmuir-Blodgett's[9] γ). Given G, x - 1 from Eq. (59) is correct within 3/4% for $1 < x < 2$. The values of I_{1Lam} obtained are in Table 3.

For the I_b = 10.9 and 374 μA cases, ϕ_{21} was unknown, so, by starting with an initial intelligent guess and iterating, I_1, I_2, V_1, and V_2 are determined so as to satisfy $\chi_1(I_1)$ from Lam's cylindrical probe theory, $\chi_2(I_2)$ from Lam's spherical probe theory, and $\phi_{21} = I_2 Z_{12}$. For I_b = 10.9 μA, $I_b = I_1 + I_2$ is also used. For I_b = 374 μA, the trial assumption is made that the case is saturated ($e|V_1| = E_b$), so V_1 = -2000 V. The value of V_3 follows from V_1 and ϕ_{31} from Table 2. The values obtained for these five quantities, for each of these two cases, are shown in Table 3. For I_b = 10.9 μA, V_3 is out of line with other values of V_3 because ϕ_{31} is out of line.

---

9. Langmuir, I. and Blodgett, K. B. (1923) Currents limited by space charge between coaxial cylinders, Phys. Rev. 22:347-356.

For beam currents from 1 through 12 μA, I_{1Lam} is seen to agree roughly with $I_b - I_2$, so Lam theory accounts for the high negative potentials of 1. The discrepancy for low values of I_b could be due to simplifying assumptions. Ions incident on the forward section have an energy $-eV_1$. At 160 km altitude and 33° latitude, returing NO^+ ions moving perpendicularly to the magnetic field have a gyro-radius of 450 (150) m at 500 (50) eV energy. For other angles, these radii are decreased by the factor sin α, where α is the pitch angle. Since the lower energy ions are more inhibited from returning by the magnetic field, perhaps this discrepancy is due to the geomagnetic field. Alternatively, the measurement of I_b may have been low at the small values, or a combination of both of these factors could have caused the discrepancy.

For beam measurements of 374 and $\sim 10^4$ μA, I_{1Lam} is seen to be much less than $I_b - I_2$, so these cases were highly saturated; most of the returning current is beam current reflected back near the sheath boundary. For the 374 μA case, this is consistent with the interpretation of Katz and Mandell,[3] Section 4.1.

4.3 Secondary Electrons and Ionization

The effect of secondary electrons is now considered briefly. The rocket surface was iridite-treated aluminum. For the ion-beam cases, values of δ, the coefficient of secondary emission of electrons, for NO^+ ions on this surface for energies up to 2 keV are needed. In lieu of this, the value assumed is .18, the yield from 1 keV O^+ ions on molybdenum.[10] All of the secondary electrons from 1 escape, so, I_{1Lam} should have been compared to $(I_b - I_2)/(1 + \delta)$. This slightly increases the discrepancy at small values of I_b. Assuming $\delta = .18$, the secondary electron density at the surface of 1 is ~ 1% of the ion density, less away from the surface, so conductor and sheath charges are affected negligibly.

The electron-beam case is much different. Using the formula of Sternglass[11] and the values for aluminum[10]: $\delta_{max} = .97$ and $U_{max} = 300$ V, $\delta = .72$ is obtained for U = 90 V. Since the secondaries have but a few eV energy, none escape, so the return current is unchanged. If all of the secondaries left the surface with 3 eV of energy, the electron density at the surface would be nine times as great as with $\delta = 0$, and the secondaries would extend ~ 1/4 m from the surface.

---

10. Stannard, P. R., Katz, I., Mandell, M. J., Cassidy, J. J., Parks, D. E., Rotenberg, M., and Steen, P. G. (1980) Analysis of the Charging of the SCATHA (P78-2) Satellite, Report NASA CR-165348, SSS-R-81-4798, pp. 22-24, 29.

11. Sternglass, E. J. (1954) Backscattering of kilovolt electrons from solids, Phys. Rev. 95:345.

Nevertheless, the magnitude of the total charge of the secondaries is small compared to $|q_s|$, so q_1 and q_s are little affected. Some incident electrons are backscattered. The number is less than the number of secondaries, and they are finally captured.

Ionization by beam and return ions is less than a few percent of the peak value due to small ion speeds, so is negligible. For the electron-beam case, however, the outward and returning beam and the return electrons from the plasma produce ionization in the sheath, especially close to the forward section. The minimum ionization mean free path (at the peak of the ionization cross section vs energy curve) is 400 m at 138 km, and 1300 m at 160 km altitude; so, it is expected to have a moderate effect at the most.[12] Since ionization constitutes an additional return current, the sheath radius must be diminished to maintain the same total return current. The effect is not treated quantitatively here. The magnetic field causes the electrons to gyrate, and thus inhibits their flow across the field. This effect is not treated quantitatively here either.

4.4 Discussion

The values of V_2 in Table 3 for ion-beam emission are relatively small and negative in qualitative agreement with the value in Case I, Table 2, of Katz and Mandell.[3] Except for I_b = 1 μA, however, they are appreciably more negative than indicated by their value. This is due mainly to taking the voltmeter current into account here. The front part of 2 had a positive surface charge density. It received most or all of the secondary electrons that went from 1 to 2. If 10% (probably much too high) of the secondaries from 1 went to 2, I_2 would be increased 19 to 33% by increasing δ from 0 to .18. The sign of the charge on the rear part of 2 may be determined by comparing the charge on 2 that is tied up in the capacitance between the two sections, with the total charge on 2. The former is the product of ϕ_{21} and this capacitance. (A value of the latter consistent with C_f', Eqs. (35) and (36), p_{ij}'s, and q_i's should be used.) The resultant product is 1.3 to 1.5 times q_2. So, the charge on the rear part of 2 is concluded to be negative, contrary to the statement of Katz and Mandell,[3] Section 3.1. Trajectories of plasma ions existed to all parts of 2 except possibly to the (unknown) wake side. The $(-.3I_2)$ plasma electron current for the 1 μA case must have reached mainly the negative surface charge density part of 2 because of the negative potential barrier near the other parts. For the -10 mA case, the

12. Leadon, R. E., Woods, A. J., Wenaas, E. P., and Klein, H. H. (1981) Analytical Investigation of Emitting Probes in an Ionized Plasma, AFGL-TR-81-0138, ADA104166, § 3.4.2.

forward and rear section potentials were of opposite signs, so there was a zero-potential surface surrounding 2 that closed on the separating insulator. As with ion-beam cases, but with opposite signs, the front part of 2 had a negative surface charge density and the rear part a positive surface charge density. Secondary electrons from 1 could not escape, and those from 2 were negligible since V_2 was so close to zero. The ionization of neutral air molecules by beam and returning electrons, here neglected, similar to increasing n_o, is expected to increase q_1 and $|q_s|$ significantly, but not to affect the conductor potentials appreciably.

4.5 Sheath Radii

Sheath radii are calculated by assuming that the plasma return current equals the thermal current density of the attracted specie times the sheath area. When the sheath is small, it is cylindrical (Figure 2), so

$$n_o e v_t (2\pi R_{sc} 2B + \pi R_{sc}^2) = I_1, \tag{61}$$

where

$$B = R_{sc}\left[1 + \left(\frac{b}{a} - 1\right)\left(\frac{a}{R_{sc}}\right)^{\frac{b}{b-a}}\right]. \tag{62}$$

The latter is the simplest expression found for the half-length of a cylinder that increases from b to R_{sc} with dB/dR_{sc} non-negative and increasing monotonically from < 1 to 1 as R_{sc} increases from $\underline{a}$ to $R_{sc} >> b$. When the sheath is large compared to the rocket, the sheath is spherical (Figure 3), so

$$n_o e v_t 4\pi R_{ss}^2 = I_1. \tag{63}$$

Except for I_b = 10.9, 374, and -10^4 μA, these sheath radii are calculated both for $I_1 = I_b - I_2$: R_{scm} & R_{ssm}, and for $I_1 = I_{1Lam}$: R_{scLam} & R_{ssLam}. The results are shown in Table 4. Column 1_m, and rows R_{scm} and R_{ssm}, are for $I_1 = I_b - I_2$. For the ion-beam cases, these would be 8 to 11% larger if δ were assumed to be .18 instead of 0. For the electron-beam case, they are unaffected by δ. With the possible exception of the I_b = 1 μA case, the probe (at R = 1.71 m) is seen to be inside the sheath. This agrees with the possible interpretation in

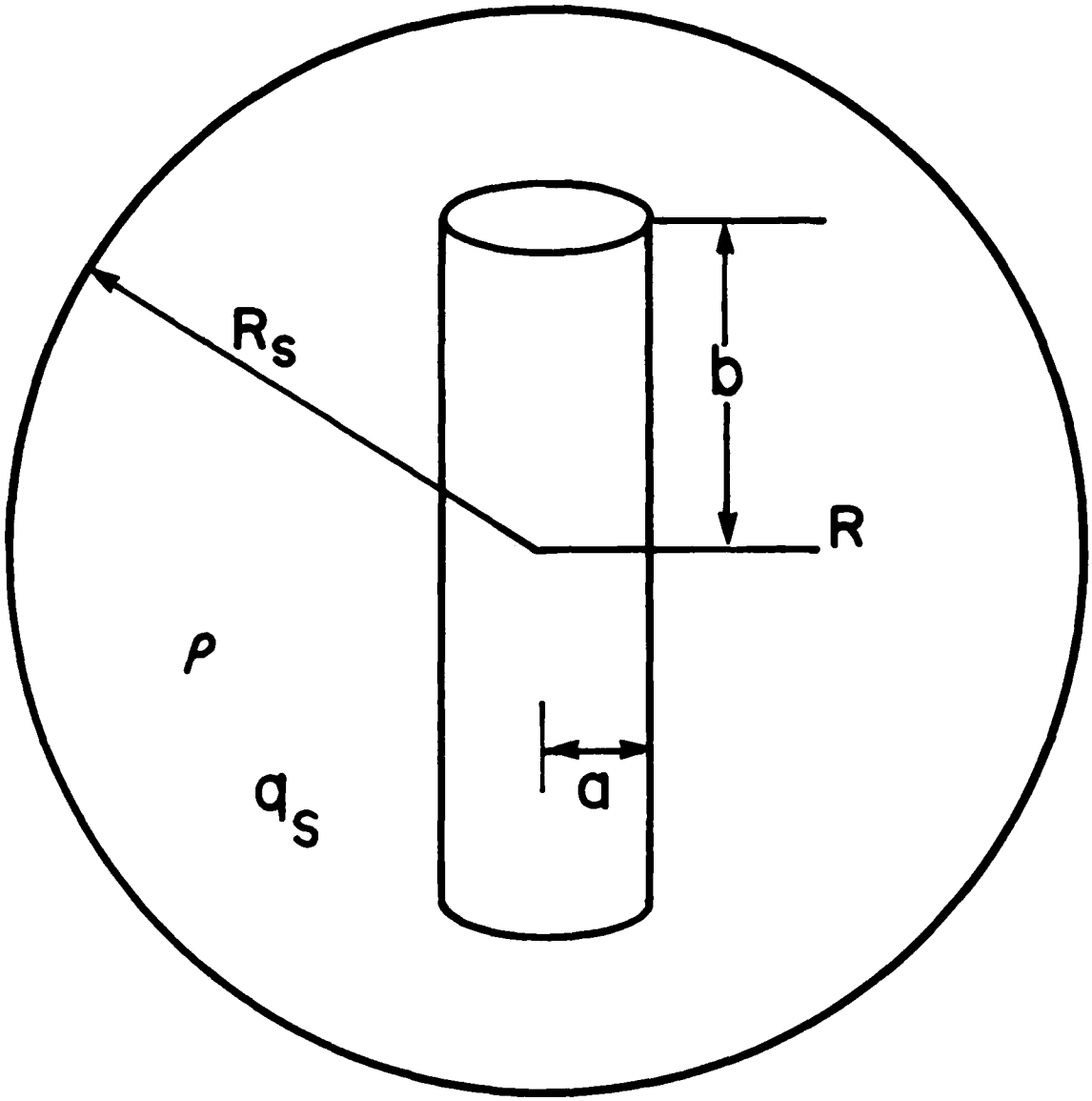

Figure 3. Cylinder With Spherical Sheath

Table 4. Sheath Radii and Sheath Potential Coefficients

I_b	1_m	1	8_a	8_b	8_c	9	10.9	12	374	-10^4	μa
I_1	.95	2.58	11.7	9.6	10.7	9.5	10.4	11.3	25.8	-853	μa
R_{scm}	1.3		4.1	4.2	4.1	4.4		5.2			m
R_{scLam}		2.3	5.2	4.7	5.0	4.7	4.9	5.1	7.9	2.8	m
R_{ssm}	1.7		4.9	4.9	4.9	5.2		6.0			m
R_{ssLam}		2.9	6.1	5.5	5.9	5.5	5.8	6.0	9.1	3.4	m
p_{1sc}	6.8	4.3	2.1	2.3	2.2	2.3	2.2	2.1	1.4	3.7	V/nC
p_{3sc}	4.0	3.6	2.0	2.2	2.1	2.2	2.1	2.0	1.4	3.3	V/nC
p_{1ss}	7.6	4.7	2.2	2.4	2.3	2.4	2.3	2.2	1.5	3.9	V/nC
p_{3ss}	5.3	4.1	2.1	2.4	2.2	2.4	2.3	2.2	1.5	3.6	V/nC
p_{1s}	7.2	4.5	2.2	2.4	2.3	2.4	2.3	2.2	1.5	3.8	V/nC
p_{3s}	4.7	4.0	2.1	2.3	2.2	2.3	2.2	2.2	1.5	3.5	V/nC

Except for the 1_m column and the I_b, R_{scm}, and R_{ssm} rows, the numbers are for $I_1 = I_{1Lam}$.

Section 4.1 of Katz and Mandell.[3] For the I_b = 1 μA case, other more realistic sheath models are tried. The distance of the sheath edge from the rocket axis along the line to the probe is calculated assuming I_1 = 2.58 μA and the sheath area equals $I_1/n_o e v_t$. For the forward section concentric with a prolate spheroid

sheath having semi-minor and semi-major axes a_e and b_e with

$$b_e = a_e\left[1 + \left(\frac{b}{a} - 1\right)\left(\frac{a}{a_e}\right)^{\frac{b}{b-a}}\right], \tag{64}$$

2.6 m is obtained. The major and rocket axes are coincident; a_e = 2.7, b_e = 3.2 m. With the same sheath, but with the forward section displaced along its axis so that its rear edge is a distance of .41 and .025 m from the sheath edge parallel to the axis, 1.6 and 1.1 m, respectively, are obtained. The last model tried is

$$r = 3.03 + 1.74\cos\theta \tag{65}$$

in a plane containing the axis rotated about the axis, the origin at the center of the forward section, and θ measured from the forward sense of the axis. For y = .025 m, 2.0 m is obtained. Thus, the probe is concluded to be at or near the sheath edge. If I_1 = 2.58 μA, the results of the different models differ too much to conclude whether or not the probe was inside or outside. If I_1 = .95 μA, the probe was almost certainly outside of the sheath.

4.6 Sheath Potential Coefficients

Values of potential per unit sheath charge due only to sheath charge, assuming a cylindrical sheath, p_{jsc}, and assuming a spherical sheath, p_{jss}, are calculated at the surface of the forward section, j = 1, and the probe, j = 3, as indicated in Appendix B. They are shown in Table 4 and are a function only of the geometry, including that of the sheath. The mean of p_{jsc} and p_{jss} is calculated, weighted according to sheath radius:

$$p_{js} = (1 - F)p_{jsc} + Fp_{jss} \tag{66}$$

$$F = \frac{R_{sc} - a_1}{R_{sc} + b_1 - 2a_1}\,. \tag{67}$$

The constants in Eq. (67) are chosen so that F = .5 when $R_{sc} = b_1$. Values of p_{js}, j = 1,3, are shown in Table 4. For I_b = 8, 9, and 12 μA, values of p_{js} for $I_1 = I_b - I_2$ differ from those for $I_1 = I_{iLam}$ by half the percentage that the latter current differs from the former (Table 3).

4.7 Conductor and Sheath Charges

The charges on the conductors and in the sheath are now obtained for each case. In steady state, the total rocket and sheath charge vanish; therefore, the sheath charge is

$$q_s = -(q_1 + q_2 + q_3). \tag{68}$$

The potential of the conductors due only to sheath charge is

$$V_{js} = p_{js} q_s, \tag{69}$$

where the approximation is made that

$$p_{2s} = p_{1s}. \tag{70}$$

From these equations and Eq. (1),

$$V = (P - P_s)Q, \tag{71}$$

where

$$p_{sij} \begin{cases} = p_{1s} \text{ for } i = 1 \text{ or } 2 \\ = p_{3s} \text{ for } i = 3. \end{cases} \tag{72}$$

So,

$$Q = (P - P_s)^{-1} V. \tag{73}$$

From Eq. (30), V in Table 3, P_s in Table 4, and Eqs. (73) and (68), the values of Q and q_s in Table 5 are calculated. Values of V_s from Eq. (69) are also given. By setting $P_s = 0$ in Eq. (73), the charges q_{i0} are obtained that the conductors would have at the same potential but with $q_s = 0$. The results are in Table 5. Except for $I_b = 1$ μA, the magnitudes of q_1 and q_2 are seen to be changed no more than 9%. So, the sheath has only a minimal effect on the conductor charges. By using Eq. (6), if the plasma, 2 and 3 were absent and the potential of 1 were unchanged, then q_{1a}, shown in Table 5, would be obtained for the charge. The results show that the presence of the rear section causes about 89% more charge to accumulate on the forward section.

Table 5. Conductor Charges and Potentials Due to the Sheath, Probe Position Potential, and Probe Current

I_b	1_m	1	8_a	8_b	8_c	9	10.9	12	374	-10^4	μA
q_1	-7.7	-6.5	-69	-51	-60	-50	-58	-66	-229	11	nC
q_2	2.2	2.5	31	23	27	23	26	30	107	-4.7	nC
q_3	-.083	-.074	-.44	-.22	-.21	-.32	.079	-.37	-1.6	-.005	nC
q_s	5.6	4.1	38	28	33	28	32	36	123	-6.6	nC
V_{1s}	40	18	83	68	76	68	73	80	182	-26	V
V_{3s}	26	16	81	66	74	66	71	78	180	-23	V
q_{1a}	-3.2	-3.2	-37	-27	-32	-27	-31	-35	-126	5.7	nC
q_{10}	-5.5	-5.5	-65	-47	-56	-47	-54	-61	-219	10	nC
q_{20}	2.8	2.8	32	24	28	24	27	31	110	-5.1	nC
q_{30}	-.047	-.047	-.30	-.11	-.081	-.20	+.20	-.24	-1.3	-.045	nC
V_3	-30	-30	-249	-137	-142	-175	-19	-217	-960	-.15	V
V_{pp1}	4.8	.76	-65	-42	-54	-42	-52	-60	-290	2.3	V
V_{pp}	4.4	.47	-66	-43	-55	-42	-51	-61	-293	2.3	V
I_{3vm}	.67	.67	11	9.7	12	8.3	16	11	35	-3.0	nA
I_{30}	(.018)	(.049)	.22	.18	.20	.18	.20	.22	.49	-16	nA
I_{3M}	(12)	(31)	1200	530	610	670	78	990	9900	-67	nA

4.8 Probe-Position Potential

If $q_3 = 0$, then V_3 is the potential of the position of the probe with the probe removed, V_{pp}. If $q_3 \neq 0$, V_{pp} may be calculated. A simple and fairly accurate method is to subtract from V_3 the part of the potential due to q_3:

$$V_{pp1} = V_3 - p_{33}q_3. \tag{74}$$

Values of this are shown in Table 5. The proper way is to argue that, if 3 were not there, the charges would be

$$Q' = (P_2 - P_{s2})^{-1}V, \tag{75}$$

where q_i', V_j have i,j = 1,2, and P_2 and P_{s2} are P and P_s with the third row and column deleted. Then

$$V_{pp} = (p_{13} - p_{3s})q_1' + (p_{23} - p_{3s})q_2'. \tag{76}$$

Values of this are also shown in Table 5. They are seen to be close to V_{pp1}, but are seen to differ greatly from V_3. This shows that $|q_3|$ was large enough to affect V_3 greatly. Except for I_b = 1 μA, there exists a value of conductance between Sections 1 and 3 (less for the ion beams, more for the electron beam than $1/Z_{31}$) for which $q_3 = 0$ so that $V_3 = V_{pp}$. This may be seen by noting that V_{pp} is between the actual V_3 (Z_{31}) and V_3 ($Z_{31} = \infty$) ~ - kT/e for ions except for I_b = 1 μA) and V_3 ($Z_{31} = 0$) = V_1 for electrons. The value of V_{pp} for the I_b = 1 μA case should be 0 or slightly negative; ~ 5 V is unphysical. Perhaps this indicates that I_b > 1 μA. If Katz and Mandell,[3] Section 4.1, meant that V_{pp} is 40% of V_1, then this disagrees with the above, since V_{pp} = 10 to 15% of V_1, except for the I_b = 1 μA and -10 ma cases.

4.9 Probe Current

In the absence of a theory for a probe in the sheath of another conductor, some limiting values of the streaming ion or electron current to 3, I_3, are calculated. Assuming no other conductance, this current is balanced by the voltmeter current

$$I_{3vm} = \phi_{31}/Z_{31}. \tag{77}$$

$Z_{31} = 3 \times 10^{10}$ Ω. Values of I_{3vm} are shown in Table 5. If 3 were at the potential V_{pp}, it would collect approximately a fraction of I_1 equal to the fraction of the equipotential surface area through it that it occupies. Assuming this equipotential surface to be a cylinder concentric with the forward section, this area is

$$A_c = 2\pi d^2 + 2\pi d2B = 70.9 \text{ m}^2. \tag{78}$$

B is given by Eq. (62), where $a = a_1$, $b = b_1$, $R_{sc} = d$, which are given in Table 1. If, instead, the surface were assumed to be a sphere concentric with 1, the area would be

$$A_s = 4\pi[d^2 + (b_1 - s)^2] = 49.6 \text{ m}^2. \tag{79}$$

The mean, $A = 60$ m^2, will be used. The approximate current collected if $V_3 = V_{pp}$ then should be

$$I_{30} = \frac{\pi a_3^2}{A} I_1 = 1.9 \times 10^{-5} I_1 . \tag{80}$$

Use of this equation yields the values in Table 5. I_{3vm} is seen to be appreciably (generally ~ 60 times) higher than I_{30} in qualitative agreement with V_3 being appreciably less (more negative) than V_{pp}. An upper bound, I_{3M}, is obtained the same way but substituting the maximum impact parameter

$$p = a_3 \sqrt{1 - \frac{eV_3}{kT}} \tag{81}$$

in place of a_3. Values of I_{3M}, also shown in Table 5, are seen to have far too large a magnitude. Except for the $I_b = -10^4$ μA case, this is mainly because Eq. (81) gives values many times the Debye length, whereas only particles with an impact parameter less than a few Debye lengths reach the probe. Also, this assumes that all field lines are radially inward to 3. Since this is incorrect, many ions with impact parameter less than the value from Eq. (81) will miss the probe. The values of I_{30} and I_{3M} for $I_b = 1$ μA have no meaning unless the probe is inside the forward section sheath. Assuming the probe to be outside of the sheath for this case, spherical Lam theory and Eqs. (38)-(46) give $i_i > \chi + 1$ for $V_3 = -30$ V. This is incorrect; Lam theory must be invalid since $\tau < 1$. A fairly accurate value, however, may be obtained from a careful extrapolation of Laframboise's[6] results for a spherical probe, as follows:

$$k_1 = 1 + .481\xi - .108\xi^2 \tag{82}$$

$$k_2 = .0331\xi + .078\xi^2 \tag{83}$$

$$-\chi = k_1(i - 1) - \frac{k_1 - 1}{k_2} \ln[1 + k_2(i - 1)]. \tag{47}$$

The four numbers in Eqs. (82) and (83) are chosen so that Eq. (47) agrees with Laframboise for $\xi = .2$ and .3 at $\chi = 25$, and for $\xi = .5$ at $\chi = 20$ and 25. Assuming that Laframboise's numbers are correct, for $0 < \xi < .5$ and $0 < \chi \leq 25$, these equations yield χ correctly probably within .2%. For $0 < \chi \leq 25$, the error is certainly less than .8% for $\xi = .2$, 1.9% for $\xi = .3$, and .4% for $\xi = .5$. Assuming $n_o = 10^9\ m^{-3}$, $\xi = .372$ and these equations give $I_3 = 16$ nA. Assuming $n_o = 5 \times 10^8\ m^{-3}$ (at the sheath edge), they give $I_3 = 8.4$ nA. This is still an order of magnitude larger than I_{3vm}. The contribution to I_3 of secondary and scattered electrons from the forward section is negligible. Perhaps this discrepancy is due to neglecting the effect of the magnetic field that decreases the return current. Alternatively, perhaps it indicates that the probe was inside the sheath where these probe theories are invalid. This would favor the larger value of I_1, for which the probe would more likely be inside the sheath. Although unlikely, it is possible that the extrapolation yields much too high a value of current.

As $|I_b|$ is increased up to the minimum value for saturation, $|V_3|$ increases. As $|I_b|$ is increased further, $|V_3|$ decreases and V_3 asymptotically approaches $\sim SkT/e$ as $|I_b| \to \infty$, where S = 1 for an ion beam, and -1 for an electron beam. The reason for $|V_3|$ decreasing is that, above minimum saturation as $|I_b|$ increases, if V_3 remained constant, I_{3vm} and the fraction of return current collected by the probe would remain constant, so the amount collected would increase and the two currents would not balance. Thus, V_3 must change to decrease the fraction collected, and to increase I_{3vm} to maintain balance. So, for a 2 keV ion beam, $|V_3|$ would be maximum at $I_b \approx 26$ μA; for a 90 eV electron beam, V_3 would be maximum at $I_b \approx -853$ μA. Since the electron-beam case has $V_3 \approx 0$, it is seen to be much more highly saturated than the $I_b = 374$ μA case.

4.10 Charging Time Constant

Now the charging time due to current and capacitance is calculated. Lowercase letters are used for instantaneous values of variables, and upper-case letters for steady-state values. The effect of the probe is neglected. Differentiating

the first two rows of Eq. (2) with respect to time, and equating to the current:

$$\dot{q}_1 = c_{11}\dot{v}_1 + c_{12}\dot{v}_2 - (c_{11} + c_{12})\dot{v}_{1s} = i_1 - I_b + \frac{v_2 - v_1}{Z_{21}} \tag{84}$$

$$\dot{q}_2 = c_{12}\dot{v}_1 + c_{22}\dot{v}_2 - (c_{12} + c_{22})\dot{v}_{1s} = i_2 - \frac{v_2 - v_1}{Z_{21}} \tag{85}$$

The assumptions are made that:

$$\dot{v}_{1s} = \frac{\dot{q}_s}{Q_s} V_{1s} = \frac{\dot{q}_1 + \dot{q}_2}{Q_1 + Q_2} V_{1s} \tag{86}$$

$$i_1 = \frac{v_1 - V_{10}}{V_1 - V_{10}} \left[I_b - \frac{V_2 - V_1}{Z_{21}} \right] \tag{87}$$

$$i_2 = \frac{v_2 - V_{20}}{V_2 - V_{20}} \times \frac{V_2 - V_1}{Z_{21}} . \tag{88}$$

Approximate values of the conductor potentials before the beam is turned on, V_{i0}, need to be known. For them, Eqs. (38) to (46) are used with I = 0 (or $(V_{20} - V_{10})/Z_{21}$). Interpolating numbers in Laframboise[6] Table 6c, V_{10} = -.214 V is obtained. Using Eqs. (47) to (49), V_{20} = -.196 V is obtained. The beam is assumed to be turned on at t = 0 and to be a step function; that is, to have a rise time much shorter than the charging times. The solution is found to be

$$q_i = Q_i + A_i e^{-t/\tau 1} + B_i e^{-t/\tau 2}. \tag{89}$$

The algebra is lengthy, and the expression for τ_j (functions of the constants in Eqs. (84) to (88), the solution of a quadratic equation) is long. One time constant is 10% (1 or 2% for I_b = 1 μA and 20% for $I_b = -10^4$ μA) of the other. Values of the larger time constant are shown in Table 6. For $n_o = 10^3$ cm^{-3}, the ion and electron plasma periods are .76 ms and 3.5 μs, respectively. The

Table 6. Charging Time Constant and Initial Ion Transit Time Through the Sheath

I_b	1_m	1	8_a	8_b	8_c	9	10.9	12	374	-10^4	μA
τ	8.0	2.6	6.0	5.4	5.7	5.4	5.6	5.9	8.8	.040	ms
$t_{ts}(\tau)$	.90					2.2		2.4	(9.4)	(.5)	ms
$t_{ts}(t_{ts})$									(13.8)	(1.4)	ms
$t_{tc}(\tau)$	.93	1.7		2.1					2.4	.19	ms
$t_{tc}(t_{tc})$										.32	ms

charging time constant is seen to be much larger. A simple, approximate way of calculating τ is given in Reference 2. Except for I_b = 374 and -10^4 μA, it gives values within 10% of those in Table 6. For I_b = 374 and -10^4 μA, the values in Reference 2 are not values of τ, which should have been 7.6 and .0078 ms, respectively, but are close to the values, .65 (assuming δ = .18) and .0012 ms, respectively, (from the simple way) of t_1, the time for the potential of the forward section first to reach $V_1 = E_b$. (v_1 then overshoots V_1 before finally settling at V_1.) Values of t_1 also could be calculated easily by the above more accurate method. At least with the simple way, τ is inversely proportional to $(1 + \delta)I_1$, so it has this dependence for such saturated cases; however, since $(1 + \delta)I_1 = I_b - I_2$ for unsaturated cases, τ is then independent of δ, given I_b. Actually, $dI_1/d(-V_1)$ for ion beams decreases with increasing $(-V_1)$; similarly, $di_1/d(-v_1)$ probably decreases with increasing (-v). Taking this into account would lead to the charging being nonexpotential. The treatment here, however, should give approximately the correct behavior.

4.11 Sheath Ion Initial Transit Time:

The approximate traverse time, t_t, is calculated for the first ions after the beam is turned on to travel radially between R_s and R_1, the assumed forward section radius. In Reference 2, the sheath was assumed spherical, and of radius equal to the value tabulated. It was concentric to a spherical conductor of .5 m radius representing the forward section. The values obtained of $t_t = t_{ts}$ for $\tau' = \tau$ or t_{ts} are shown in Table 6. Those for I_b = 374 and -10^4 μA should be discounted. They are much too large because the values of R_s are too large. Now the sheath is assumed cylindrical and concentric with the actual forward section, Figure 2. For the ion-beam cases, the ion is at $R = R_{sc}$ with $\dot{R} = -v_{ti}$ at t = 0. Eq. (A28), Appendix C, is integrated numerically to $t = t_t(\tau')$ where $R = a_1$. For the electron-beam case, the ion is at $R = a_1$ and $\dot{R} = 0$ at t = 0; Eq. (A28) is integrated numerically to $t_t(\tau')$ where $R = R_{sc}$. Some results for $t_t = t_{tc}$ and $\tau' = \tau$ or t_{tc} are shown in Table 6. The values of $I_b = 8_b$ and 9 μA are expected to be nearly identical. The results for the two models are seen to be about the same. The values for t_t for a spherical sheath around the cylindrical forward section, Figure 3, would be a little larger since $R_{ss} - a_1$ is larger than $R_{sc} - a_1$. t_t is seen to be smaller than τ except for the I_b = -10 ma case. So, τ is the minimum time in the ion-beam cases, and .32 ms in the electron-beam case, for steady state to be reached.

5. CONCLUSIONS

The charging data are analyzed for eight positive ion cases, and one electron-beam emission case, from a three-conductor rocket in the lower F-region at night. Calculation of sheath radii show that the spherical emissive probe was in the sheath of the forward section, in agreement with Katz and Mandell's interpretation,[3] although the I_b = 1 μA beam current case is a possible, but unlikely, exception. How potential coefficients for any number of conductors can be measured is indicated. Since the coefficients were not measured for the rocket, and the geometry was sufficiently simple, values of them and of sheath potential coefficients, both dependent only on the geometry, are calculated fairly accurately. An empirical formula found for the potential due to a charged conducting cylinder, Smythe's charge distribution on a conducting cylinder, his empirical formula for the capacitance, and three gedanken experiments are used to determine these coefficients.

By using these coefficients, understanding was gained; this included the charge on the conductors and in the sheath, the potential at the position of the probe without the probe, V_{pp}, and the charging time constant.

An empirical formula accurate to .2 to 4% in different ranges of probe radius to Debye length ratio, ε, up to 5 is found for Laframboise's spherical probe results. Empirical formulae accurate to 1% over the whole range are found for F and G. F is useful in Lam's theory, and in lieu of $(-\alpha)^2$ in Langmuir-Blodgett's spherical probe theory. G is useful in Lam's theory, and in lieu of $(-\beta)^2$ in Langmuir-Blodgett's cylindrical probe theory.

The spherical probe theories of Laframboise and Lam, and I_2, the rear section voltmeter current, lead to the potential, V_2, of the rear section. The values are negative and, since the contributions from the various charges nearly cancel, are of small magnitude in qualitative agreement with a relevant calculated value by Katz and Mandell. In general, however, the magnitudes are appreciably larger due to voltmeter conductance. These and measurements of ϕ_{i1}, give absolute values of potential of the forward section, V_1, and probe, V_3. For ion-beam cases, the front part of the rear section is concluded to have a positive surface charge density, and the rear part a negative surface charge density. The latter disagrees with Katz and Mandell. Values of return current are calculated from V_1 by using Lam's probe theory for a cylinder. Except for the two high-beam current (374 and -10^4 μA) cases, they agree roughly with $I_b - I_2$. So, probe theory accounts for the high value of $|V_1|$ for these unsaturated cases ($e|V_1| < E_b$, the particle energy of the beam). It also shows that the two high-beam current cases, especially the electron case, are highly saturated (I_b much greater than necessary for $e|V_1| = E_b$); most of the beam current is reflected near the sheath edge back to the forward section.

For the ion-beam cases, although all secondary electrons from the forward section escape, it appears that they have a negligible effect, other than decreasing the return current and sheath radius slightly. For the electron-beam case, many secondary and scattered electrons come from the forward section surface, but they cannot escape, and have very little effect, even on the sheath charge density. The effect of ionization by ions is negligible, that by electrons is expected to be small to moderate, and the effect of magnetic field on electrons is expected to be quite appreciable.

Values of charge on the rocket conductors and in the sheath are calculated. They are not greatly changed by the sheath charge. The charge on the rear section must always have the opposite sign and a smaller magnitude than that on the forward section. The presence of the rear section is found to increase the charge on the forward section by about 89%. The potential of a conductor is concluded to be determined mainly by the current from it, and the charge on it to be determined by potentials and induction (coupling). Both a simple and an accurate way are used to calculate V_{pp}. It is much higher (less negative) than V_3. This is due to q_3, the charge on the probe (that is related to the equilibrium probe current). V_{pp} is 10% to 15% of V_1, rather than 40% as apparently interpreted by Katz and Mandell. For each ion-beam case, except 1 μA, a value of probe voltmeter resistance exists for which q_3 would equal 0, and V_{pp} would equal V_3. Upper and lower limits of probe current from the plasma are calculated that bracket the balancing probe voltmeter current, I_{3vm}. For I_b = 1 μA, the value of return current to the probe calculated by probe theory is an order of magnitude larger than I_{3vm}. This is probably due to neglecting the effect of the magnetic field, but may also be due to plasma current to the forward section, and electric field from the forward section, i.e., to the probe being inside of the forward section sheath. As the beam current increases beyond minimum saturation, V_3 approaches zero and, then, at extreme values, kT/e beyond zero. The electron-beam case is in accordance with this; further verification would be desirable.

The charging time constant due to capacitance is an order of magnitude larger than the plasma period, and, except for the electron-beam case, is larger than the initial ion transit time through the steady-state sheath. So, the minimum time to reach steady state is determined by the charging time due to capacitance for an ion beam, and by the ion transit time, a third of a ms, for the electron-beam case. The time for the 374 or -10^4 μA case to become saturated was less than a plasma period.

In spite of many approximations, this analysis is believed to be qualitatively and approximately quantitatively correct, at least for the ion-beam cases. Since $\xi < 10$ for the cases here, a better probe theory than Lam's, perhaps that of Bernstein and Rabinowitz,[13] should be used for potentials out of range of those of Laframboise.

---

13. Bernstein, I. B., and Rabinowitz, I. (1959) Theory of electrostatic probes in a low density plasma, Phys. Fluids 2:112-121.

For the electron-beam case, a treatment is needed that includes the effect of magnetic field, and probably ionization, for reliable results. An accurate (numerical) solution of Poisson's equation would make an interesting and perhaps valuable comparison with the results in this report. The analysis techniques used here, applied to a greater variety of data, should produce much more understanding.

From the results in this report, and those of Lam-Jaycor,[12] one may induce the following general steady-state properties of vehicles in the ionosphere at potentials small enough not to cause breakdown or appreciable ionization of background neutrals. For a given beam current and shape of vehicle with an all-conducting surface, as the size increases, the sheath thickness, vehicle potential, and charge decrease. For sheaths that are thick compared to vehicle size, the charge decreases very little. For a given beam current and vehicle, as the fraction of the surface that is covered with dielectric is increased, the potential and charge on the conducting part increase.

It is hoped that this report will provide useful considerations and techniques, and/or stimulate ideas leading to better ones for experiments and analyses of object-charging in laboratory and space plasmas.

References

1. Cohen, H. A., Sherman, C., and Mullen, E. G. (1979) Spacecraft charging due to positive ion emission: an experimental study, G.R.L. 6:5-15.

2. Dubs, C. (12 Nov. 1982) Potentials and Charges on Conducting Rocket Sections, AFGL-TR-82-0349, ADA130143.

3. Katz, I., and Mandell, M. J. (1982) Differential charging of high-voltage spacecraft: the equilibrium potential of insulated surfaces, J.G.R., 87:4533-4541.

4. Smythe, W. R. (1962) Charged right circular cylinder, J. Appl. Phys. 33:2966-2967.

5. Page, L. (1935) Introduction to Theoretical Physics, Van Nostrand Co., New York, Second Edition, § 120.

6. Laframboise, J. G. (1966) Theory of spherical and cylindrical Langmuir probes in a collisionless, Maxwellian plasma at rest, UTIAS Report No. 100.

7. Lam, S. H. (1965) Unified theory for the Langmuir probe in a collisionless plasma, Phys. Fluids 8:73-87.

8. Langmuir, I. and Blodgett, K. B. (1924) Currents limited by space charge between concentric spheres, Phys. Rev. 24:49-59.

9. Langmuir, I. and Blodgett, K. B. (1923) Currents limited by space charge between coaxial cylinders, Phys. Rev. 22:347-356.

10. Stannard, P. R., Katz, I., Mandell, M. J., Cassidy, J. J., Parks, D. E., Rotenberg, M., and Steen, P. G. (1980) Analysis of the Charging of the SCATHA (P78-2) Satellite, Report NASA CR-165348, SSS-R-81-4798, pp. 22-24, 29.

11. Sternglass, E. J. (1954) Backscattering of kilovolt electrons from solids, Phys. Rev. 95:345.

12. Leadon, R. E., Woods, A. J., Wenaas, E. P., and Klein, H. H. (1981) Analytical Investigation of Emitting Probes in an Ionized Plasma, AFGL-TR-81-0138, ADA104166, § 3.4.2.

13. Bernstein, I. B., and Rabinowitz, I. (1959) Theory of electrostatic probes in a low density plasma, Phys. Fluids 2:112-121.

Appendix A

Potential Due to a Charged Conducting Cylinder

The following is an empirical formula for the potential of a point R, z (see Figure 2) due to a conducting right, circular, cylinder of radius a with a charge q, b > a, R ≥ a:

$$V = g\frac{kq}{a}\left[\left(1 + \frac{b}{R\sqrt{1 + \frac{z^4}{2b^4 + R^2z^2}}}\right)^{\frac{a}{kb}} - 1\right], \qquad \text{(A1)}$$

a in meter, q in Coulomb, V in Volt.

When $b \ll |z|$ and $b^2 \lesssim R|z|$,

$$V = g\frac{q}{R\sqrt{1 + \frac{z^4}{2b^4 + R^2z^2}}}. \qquad \text{(A2)}$$

When ($b \ll |z|$ and $b \lesssim R$) or $b \ll R$,

$$V = g \frac{q}{\sqrt{R^2 + z^2}} . \tag{A3}$$

When $\frac{R}{b} << \ln \frac{b}{R} << \frac{2kb}{a}$ and $|z| \lesssim b$,

$$V = g \frac{q}{b} \ln \frac{b}{R\sqrt{1 + \frac{z^4}{2b^4}}} . \tag{A4}$$

When $z = 0$, $R = a$, $k = 1.777$, and $a/2 \leq b \leq 8a$, then q/V is within 1.25% of the correct capacitance.

p_{103}^{-1} is q/V obtained from Eq. (A1) with $a = .19$ m, $k = 1.777$, $b = 1.27$ m, $R = 1.71$ m, $z = 1.01$ m giving

$$p_{103}^{-1} = .260_5 \text{ nf.} \tag{A5}$$

p_{123}^{-1} is q/V obtained from Eq. (A1) with $a = .19$ m, $k = 1.777$, $b = 1.475$ m, $R = 1.71$ m, $|z| = .805$ m, giving

$$p_{123}^{-1} = .261_6 \text{ nf.} \tag{A6}$$

Appendix B

Potential Due to the Sheath

B.1. Cylindrical Sheath

The potential at R on the median plane z = 0 due to a cylindrical sheath (Figure 2) is calculated. From Eq. (A1), the potential due to an infinitesimal cylindrical shell at R' ≤ R and z' is

$$dV_{<} = g\frac{kdq_s}{R'}\left[\left(1 + \frac{z'}{R}\right)^{\frac{R'}{kz'}} - 1\right], \tag{A7}$$

where

$$z' = R'\left[1 + \left(\frac{b}{a} - 1\right)\left(\frac{a}{R'}\right)^{\frac{b}{b-a}}\right]. \tag{A8}$$

In this section, $a = a_1$ and $b = b_1$.

The potential due to a shell at R' ≥ R is assumed to be

$$dV_{>} = g\frac{kdq_s}{R'}\left[\left(1 + \frac{z'}{R'}\right)^{\frac{R'}{kz'}} - 1\right], \tag{A9}$$

This implies that the charge distribution is that for a conducting shell. The sheath volume is

$$\text{Vol} = \pi R_s^2 2B - \pi a^2 2b, \tag{A10}$$

where B is given by Eq. (62).

$$dq_s = \frac{dVol}{Vol} q_s = 2\pi\rho\left[3 + \left(2\frac{b}{a} - 3\right)\left(\frac{a}{R'}\right)^{\frac{b}{b-a}}\right] R'^2 dR', \tag{A11}$$

where

$$2\pi\rho[R_s^2 B - a^2 b] = q_s \ . \tag{A12}$$

This assumes that the average charge density, ρ, is the same in each shell volume. Errors due to this assumption are believed to be small since Laframboise,[6] Figure 33, shows ρ to be nearly constant in the sheath for $\xi = 2$ ($\pm$ 13% to $4\lambda_D$) and 5 ($\pm$9% to $8\lambda_D$ from the probe surface) and since q_1 and q_2 are not greatly changed by neglecting the plasma charge entirely. The potential due to each shell is of the form

$$dV_< = 2\pi g k \rho u(R', R) dR' \tag{A13}$$

$$dV_> = 2\pi g k \rho w(R') dR'. \tag{A14}$$

Empirical formulae are found for u and w:

$$u(R', 1.71) = .008 + .47R' + .648R'^2 \tag{A15}$$

$$w(R') = .247 + 1.427R'. \tag{A16}$$

Eq. (A15) is correct within 1% for $.19 \leq R' \leq 1.71$ m. Eq. (A16) is correct within 9% for $.19 \leq R' \leq .3$ m and within 2% for $.3$ m $\leq R'$.

The potential per unit sheath charge at the side of the rocket due only to sheath charge is taken to be

$$p_{lsc} = \int_a^{R_{sc}} dV_> / q_s. \tag{A17}$$

The potential per unit sheath charge at the probe due only to sheath charge is taken to be

$$p_{3sc} = \int_a^{1.71} dV_< / q_s + \int_{1.71}^{R_{sc}} dV_> / q_s \tag{A18}$$

for the probe inside of the sheath and

$$p_{3sc} = \int_a^{R_{sc}} dV_< / q_s \tag{A19}$$

for the probe outside of the sheath (only used for $I_b = 1_m$ μA).

B.2. Spherical Sheath

As R_s increases, the sheath boundary becomes less cylindrical and more spherical. For $R_s >> b$, this boundary (Figure 3) is nearly spherical, so is assumed spherical. The potential per unit sheath charge at the side of the rocket due only to sheath charge is taken to be

$$p_{lss} = V_{ss}(a)/q_s, \tag{A20}$$

and that at the probe is taken to be

$$p_{3ss} = V_{ss}(1.71)/q_s, \tag{A21}$$

where $V_{ss}(R)$ is derived on pp. 34 and 35 of Reference 2 and given in Eqs. (A35)-(A37) there.

Appendix C

Initial Ion Transit Time Through the Sheath

First, the potential, V(R), is calculated in the sheath at a radius R, along a radial line passing through the center of the forward section (z = 0). It is the sum of the potential at R due to q_s, q_1, and q_2 (the effect of q_3 is small and is ignored):

$$V(R) = 2\pi g k_0 \left[\int_a^R u(R',R)dR' + \int_R^{R_{sc}} w(R')dR'\right]$$

$$+ g\frac{kq_1}{a}\left[\left(1 + \frac{b_1}{R}\right)^{\frac{a}{kb_1}} - 1\right] + g\frac{kq_2}{a}\left[\left(1 + \frac{b_2}{RS}\right)^{\frac{a}{kb_2}} - 1\right] \qquad \text{(A22)}$$

from Eqs. (A1), (A13), and (A14), where

$$S \equiv \sqrt{1 + \frac{(b_1 + b_2)^4}{2b_2^4 + R^2(b_1 + b_2)^2}} \; . \qquad \text{(A23)}$$

The electric field is assumed to increase everywhere exponentially with time, t, after beam turn on with a time constant τ'. So

$$E(R,t) = -\frac{\partial V}{\partial R}\left[1 - e^{-t/\tau'}\right]$$

$$= g\left\{-2\pi k\frac{q_s}{Vol}\, I(R) + \frac{q_1}{R^2\left(1 + \frac{b_1}{R}\right)^{1 - \frac{a}{kb_1}}} + \frac{q_2}{R^2\left(1 + \frac{b_2}{RS}\right)^{1 - \frac{a}{kb_2}}}\right.$$

$$\left. \times \frac{\left[2b_2^4 + R^2\left(b_1 + b_2\right)^2\right]^2 + 2b_2^4\left(b_1 + b_2\right)^4}{\left[2b_2^4 + R^2\left(b_1 + b_2\right)^2\right]^2 S^3}\left[1 - e^{-t/\tau'}\right]\right. \tag{A24}$$

where

$$I(R) = \int_a^R \frac{\partial u}{\partial R}\, dR', \tag{A25}$$

and

$$u(R,R) - w(R) = 0. \tag{A26}$$

The empirical formula

$$\left.\begin{aligned} I(R) &= -A(R - a) - B\ \ln\frac{R}{a} + C\left(\frac{1}{a} - \frac{1}{R}\right), \\ A &= .4347,\ B = .02784,\ C = .02093 \end{aligned}\right\} \tag{A27}$$

is accurate to .3%. The equation of motion is

$$\ddot{R} = \frac{e}{M}\, E(R,t), \tag{A28}$$

where e and M are the magnitude of charge and the mass respectively of the ion, assumed to be NO^+.

END

9-87

DTIC